

Estimation of Weather Noise in Coupled Ocean–Atmosphere Systems Using Initialized Simulations[Ⓞ]

JIESHUN ZHU^a

Key Laboratory of Meteorological Disaster, Ministry of Education/Joint International Research Laboratory of Climate and Environment Change/Collaborative Innovation Center on Forecast and Evaluation of Meteorological Disasters, Nanjing University of Information Science and Technology, Nanjing, China

JAGADISH SHUKLA

Center for Ocean–Land–Atmosphere Studies, Department of Atmospheric, Oceanic, and Earth Sciences, College of Science, George Mason University, Fairfax, Virginia

(Manuscript received 20 October 2015, in final form 8 March 2016)

ABSTRACT

This study presents a new method to estimate atmospheric weather noise from coupled models, which is based on initialized simulations with a CGCM. In this method, the weather noise is estimated by removing the signal part, as determined from the coupled ensemble mean simulations. The weather noise estimated from coupled models is compared with that estimated from uncoupled AGCM simulations. The model used in this study is CFSv2. The initialized simulations start from each April during 1982–2009 paired with four members and extend for 6 months. To make a clear comparison between weather noise in coupled and uncoupled simulations, a set of uncoupled AGCM (the atmospheric component of CFSv2) simulations are conducted, which are forced by the daily mean SSTs from the above initialized CGCM simulations. The comparison indicates that, over the Asia–Pacific monsoon region where the local air–sea coupling is important, the noise variances are generally reduced as a result of air–sea coupling, as are the total and signal variances. This result stands in contrast to the results of previous studies that suggested that the noise variance for coupled and uncoupled models is the same. It is shown that the previous conclusion is simply an artifact of the assumption applied in the AGCM-based approach (i.e., the signal is the same between coupled and uncoupled simulations). In addition, the variance difference also exhibits a clear seasonality, with a larger difference over the monsoon region appearing toward boreal summer. Another set of AGCM experiments forced by the same SST suggests that the CGCM-based method generally remains valid in estimating weather noise within 2 months of its initial start.

1. Introduction

It was identified around 40 years ago that the low-frequency ocean response is selectively amplified when the ocean is forced stochastically by fluxes representing

weather noise (Hasselmann 1976; Frankignoul and Hasselmann 1977). The phenomenon suggests a mechanism explaining low-frequency sea surface temperature (SST) variability (Sarachik et al. 1996). To explore what fractions of regional SST variability could be explained by this mechanism, it is necessary to extract weather noise surface fluxes from coupled systems either in observations or in models. One approach for this purpose is to use a linear statistical atmospheric model to remove the SST-related patterns from the observed or simulated full fields. Kleeman and Moore (1997) used this approach to estimate the noise component of the surface wind stress as a residual. Eckert and Latif (1997) additionally applied a high-pass filter to the residual. The approach has been widely applied in examining the role of the weather noise forcing in El

[Ⓞ] Supplemental information related to this paper is available at the Journals Online website: <http://dx.doi.org/10.1175/JCLI-D-15-0737.s1>.

^a Current affiliation: NOAA/Climate Prediction Center, College Park, Maryland.

Corresponding author address: Dr. Jieshun Zhu, Climate Prediction Center, 5830 University Research Court, College Park, MD 20740.

E-mail: jieshun.zhu@noaa.gov

Niño–Southern Oscillation (ENSO) irregularity and predictability by intermediate coupled atmosphere–ocean models (e.g., [Kleeman and Moore 1997](#); [Eckert and Latif 1997](#)).

Clearly, the above statistical method is far too simple to represent the complex relationship between SST and the overlying atmosphere, and, consequently, the derived noise still could be highly correlated with SST. As a significant advancement, [Schneider and Fan \(2007\)](#) presented a dynamical method to estimate weather noise. The method is based on atmospheric general circulation models (AGCMs), and the weather noise is determined by removing the forced response as determined from the uncoupled ensemble. Compared with the statistical method, the AGCM-based method has the advantage of determining both linear and nonlinear responses to SST and also the delayed atmospheric response to SST at different time lags. The method has been used to address important questions about the effect of weather noise on low-frequency SST variability, in both a perfect model framework ([Schneider and Fan 2007](#)) and observations ([Fan and Schneider 2012](#)).

In this paper, we present a new conceptual definition of weather noise. We propose that calculation of weather noise based on uncoupled forced AGCM simulations cannot properly account for the atmosphere–ocean coupling, which necessarily affects the estimation of both signal and noise in coupled simulations. A major assumption in the AGCM-based approach is that, given the large heat capacity of the ocean, its response to the atmospheric forcing is much smaller and slower. In fact, in all uncoupled AGCM runs, the ocean heat capacity is assumed to be infinitely large and the prescribed SST does not respond to the AGCM change at all. Although this assumption is valid in areas where SST fluctuations are largely determined by the oceanic dynamics, such as the eastern tropical Pacific Ocean, it is not valid in areas where the atmospheric forcing and local air–sea feedback have a strong effect on SST. For example, in the “warm seas” like the western Pacific and the Indian Ocean, SST fluctuations are affected by the atmospheric fluctuations, which in turn modify the atmospheric systems that generate them in the first place. This kind of feedback can be important to produce relatively long-living and potentially predictable signals in the ocean–atmosphere system. In such situations, it is conceivable that a prescribed SST anomaly, without responding to any feedback, is likely to exaggerate its influence on the atmosphere. Therefore, by confusing cause and effect, the uncoupled AGCM runs could result in a bias toward artificially too high variance in the air–sea fluxes ([Frankignoul 1999](#)).

To alleviate the above disadvantages in the AGCM-based approach, this study presents a new method for estimating weather noise in the coupled models. The new method can be regarded as an extension of the dynamical method of [Schneider and Fan \(2007\)](#), using coupled ocean–atmosphere general circulation models (CGCMs) instead of AGCMs. In this method, signal is defined as the ensemble average of multiple initialized CGCM simulations and noise is defined as the departure from the ensemble mean (i.e., the signal part). By applying the CGCM-based method, we also address another scientific question; that is, are the statistics of weather noise the same between the coupled and uncoupled simulations? Recently, based on the AGCM-based approach in the perfect model framework, [Chen et al. \(2013\)](#) claimed that “the weather-noise variance is generally not distinguishable between the coupled and uncoupled simulations,” a picture corresponding exactly to the assumptions in the simple stochastically forced, linear model of [Barsugli and Battisti \(1998\)](#). On the other hand, they attributed the variance difference in the full fields between the coupled and uncoupled simulations to the “constructive or destructive interference between the SST forced response and weather noise in the coupled model.” To make a clear comparison between coupled and uncoupled simulations and to be able to repeat the calculations by [Schneider and Fan \(2007\)](#), a set of uncoupled AGCM (the atmospheric component of CGCM) simulations are conducted, which are forced by the daily mean SSTs from the above initialized CGCM simulations. By comparing the CGCM and AGCM runs, the effect of coupling on the properties of weather noise will be examined.

It should be noted that, even though as far as we know no coupled attempts were made to extract weather noise from coupled systems, there were studies addressing weather noise in coupled GCMs. The interactive ensemble (IE) coupling strategy ([Kirtman and Shukla 2002](#)) is one of these examples. The technique is to use multiple realizations of the atmospheric GCM coupled to a single realization of the ocean GCM. It is based on the assumption that the AGCM has unrealistic internal dynamics noise and that an ensemble average of multiple atmospheric states forced by the same SST will reduce the internal atmospheric noise, thereby enhancing the relative strength of the SST forced signal. Experiments suggested that the IE technique dramatically improved the simulation of ENSO, the global teleconnection associated with ENSO, and the ENSO–monsoon relationship in a CGCM ([Kirtman and Shukla 2002](#)). Furthermore, the IE technique was also the underpinning of studies by [Schneider and Fan \(2007\)](#) and [Fan and Schneider \(2012\)](#), who explored the role of

TABLE 1. Description of experiments (and noise sets).

Name	Descriptions
CGCM	Initialized CGCM integrations, four members differing by four AICs
AGCM	Forced AGCM integrations, four members by using four SSTs from CGCM paired with four AICs
AGCM_1sst	As in AGCM, but using the SST from the first member of CGCM integrations, paired with four AICs
CGCM_Sagcm	As in CGCM, but the signal part is defined as AGCM ensemble mean

noise in producing surface climate variability by forcing an IE CGCM with the externally calculated weather noise fluxes. The new approach to estimate weather noise using coupled models is consistent with the underlying motivation of IE technique to reduce the artificially high noise in uncoupled AGCM simulations.

2. Models, experiments, and diagnostics

The coupled model used in this study is the NCEP Climate Forecast System, version 2 (CFSv2; Saha et al. 2014). In CFSv2, the ocean model is the Geophysical Fluid Dynamics Laboratory (GFDL) Modular Ocean Model (MOM), version 4, which is configured for the global ocean with a horizontal grid of $0.5^\circ \times 0.5^\circ$ poleward of 30°S and 30°N and a meridional resolution increasing gradually to 0.25° between 10°S and 10°N . The vertical coordinate is geopotential height (z -) with 40 levels (27 of them in the upper 400 m). The maximum depth is approximately 4.5 km. The atmospheric model is a lower-resolution version of the Global Forecast System (GFS), which has a horizontal resolution at T126 (105-km grid spacing) and 64 vertical levels in a hybrid sigma–pressure coordinate. The oceanic and atmospheric components exchange surface momentum, heat, and freshwater fluxes, as well as SST, every 30 min.

In the initialized CFSv2 simulations (referred to as CGCM; Table 1), the ocean initial conditions (OICs) are based on the instantaneous states from the European Centre for Medium-Range Weather Forecasts (ECMWF) Ocean Reanalysis System 4 (ORAS4; Balmaseda et al. 2013). CFSv2 integrations start from each April during 1982–2009 and extend for 6 months (i.e., from April to September). For each OIC, four ensemble members are generated by changing their atmospheric and land initial conditions (AICs), which are the instantaneous fields from 0000 UTC of the first four days in April of each year in the NCEP Climate Forecast System Reanalysis (CFSR; Saha et al. 2010). In a previous study, we compared the impact of CFSR and ORAS4 ocean initial conditions and found that using ORAS4 ocean initial conditions in CFSv2 produces better predictions of SST, especially in the eastern Pacific (Zhu et al. 2012).

For the application of the AGCM-based noise estimation method (referred to as AGCM; Table 1), the daily mean SSTs from the above initialized CFSv2 simulations are used to drive GFS, the identical atmospheric model in CFSv2. In the AGCM run, there are also four ensemble members. For each member (e.g., the second April case), GFS is initialized from the same atmospheric and land initial conditions as in CGCM and forced by the daily mean SST from the corresponding CGCM run. As a result, the SSTs are identical between CGCM and AGCM on the daily time scale, and their atmospheric models are also identical. The only difference is the high-frequency coupling process in CGCM, where air–sea fluxes exchange every 30 min. The two carefully designed experiments have been used to explore the role of air–sea coupling in seasonal prediction of Asia–Pacific summer monsoon rainfall (Zhu and Shukla 2013) and simulations of the boreal summer intraseasonal oscillation over India and the western Pacific (Shukla and Zhu 2014).

As expected, however, SSTs from the initialized CGCM simulations diverge with the increase in lead time (Zhu et al. 2013). To explore its effect on the weather noise estimation, a third set of experiments (referred to as AGCM_1sst; Table 1) are further conducted. In AGCM_1sst, all settings are the same as AGCM, except that AGCM_1sst is driven by the same SST for all four members (specifically chosen from the first member of CGCM). By comparing AGCM_1sst with AGCM, we estimate the “efficient period” when the SST divergence would not significantly affect the statistics of estimated weather noise and the CGCM-based method would remain valid.

In the AGCM-based approach (Schneider and Fan 2007), it was assumed that the signal component was the same between coupled and uncoupled integrations. To explore the effect of this assumption on the properties of estimated weather noise, to be able to repeat the calculations, and to reproduce the previous results, a fourth set of noise (referred to as CGCM_Sagcm; Table 1) is estimated, which is defined by removing the AGCM ensemble mean (i.e., the AGCM signal) from the full CGCM fields.

In this study, all analyses are based on 28 years (1982–2009) and presented over the Asia–Pacific monsoon region where the crucial role of local air–sea coupling has been identified (e.g., Wu and Kirtman 2004, 2007; Wang et al. 2005; Zhu and Shukla 2013). Our diagnostics are focused on surface flux variables, such as precipitation, latent heat flux, and wind stress, because it is their noise components that are thought to directly drive low-frequency SST variability (Hasselmann 1976; Frankignoul and Hasselmann 1977). The monthly mean data with the annual cycle removed are analyzed. The F test is used to determine the statistical significance of variance difference. The corresponding degrees of freedom (DOF) are 27 in our analyses.

3. Results

First, we compare the variances of full fields in CGCM with those in AGCM in May (corresponding to a 1-month lead time), for which the variances [or standard deviations (STDs)] in each ensemble member are calculated first, and then their average is applied. Figure 1 shows their STD for precipitation, surface latent heat flux (LHF), net surface shortwave flux (NSWF), and zonal surface wind stress (Taux). Consistent with previous results (e.g., Barsugli and Battisti 1998; Chen et al. 2013), the total variances for all the flux variables are clearly larger in the uncoupled AGCM than in the CGCM simulations over the monsoon region. This difference suggests a basic effect from air–sea coupling (i.e., decreasing the energy flux between atmosphere and ocean; Barsugli and Battisti 1998). In the uncoupled AGCM runs, SST does not respond to atmospheric fluctuations but exaggerates its influence on the atmosphere and results in a bias toward positive feedback (Frankignoul 1999), which increases the variances of fluxes at the air–sea interface (Barsugli and Battisti 1998).

The above variance difference between AGCM and CGCM is also evident in the signal component (Fig. 2), which is defined as their respective ensemble means. In fact, for all the four flux variables in both CGCM and AGCM, the variance distributions resemble closely those of their corresponding full fields, but with reduced amplitudes (Fig. 1 vs Fig. 2). For example, in both full and signal fields of CGCM there are large variances of precipitation and NSWF on the western coast of India and the northeastern part of the Bay of Bengal, and at two slightly shifted regions, LHF and Taux also present large variances. In AGCM, the two regions are connected by large variances for all four flux variables in both their full and signal fields. Large variances also appear in the tropical western Pacific (TWP), which is a striking difference relative to CGCM. The TWP difference between

AGCM and CGCM is actually shown in the summer season as well [e.g., the monsoon rainfall as shown by Fig. 2 in Zhu and Shukla (2013)], but it shifts slightly northward because of the seasonal cycle. Therefore, similar to the total variance (Fig. 1), the variance of signal component (Fig. 2) is also reduced as a result of air–sea coupling. We show later that differences in the signal variance in coupled and uncoupled simulations are an important factor in this study because the previous estimation of weather noise by Schneider and Fan (2007) assumed that the signal variance is the same in coupled and uncoupled simulations.

By removing the above signal component from the full field, the noise part could be derived as the residual. Figure 3 shows the STD of noise fields in CGCM and AGCM and those in CGCM_Sagcm, which are defined by removing the AGCM ensemble mean following the procedure applied in the AGCM-based approach (Schneider and Fan 2007). From Figs. 1, 2, and 3, it is evident that the variance distributions for all four flux variables are rather similar among their full, signal, and noise fields, respectively, but with different amplitudes. The comparison of the STD amplitudes between CGCM and AGCM [Figs. 3 (left) vs (right)] indicates that, as in full and signal fields, the noise variances are also reduced as a result of air–sea coupling. Further, if comparing CGCM_Sagcm with CGCM and AGCM [Figs. 3 (center) vs (left) and (center) vs (right)], it can be seen that the noise variance distributions are almost the same between CGCM_Sagcm and AGCM, but both show clearly larger amplitudes than CGCM. A good example for such difference is over the TWP, where large noise variances are clearly present in both CGCM_Sagcm and AGCM but absent in CGCM. This reproduces the results of Chen et al. (2013) that the derived weather noise variance is generally not distinguishable between CGCM and AGCM by making their assumption that the signal component is the same for coupled and uncoupled simulations. Considering that local air–sea coupling is important over the Asia–Pacific monsoon region (Fig. 2), our results suggest that the AGCM-based approach may not be appropriate to estimate signal and noise.

The above variance difference could be quantitatively examined by the F test. Figure 4 presents the STD ratio of the full, signal, and noise fields, with significant difference highlighted in colors. Figure 4 clearly shows that, for all the four flux variables, ratio distributions are similar for all three fields (full, signal, and noise fields). For instance, their variances derived from full, signal, and noise flux fields are consistently reduced by air–sea coupling over the TWP at the 99% confidence level. Reduced variances also appear in the northern Indian Ocean, with higher confidence in LHF than other flux

Standard Deviation of full Fields (May: 1-Month Lead)

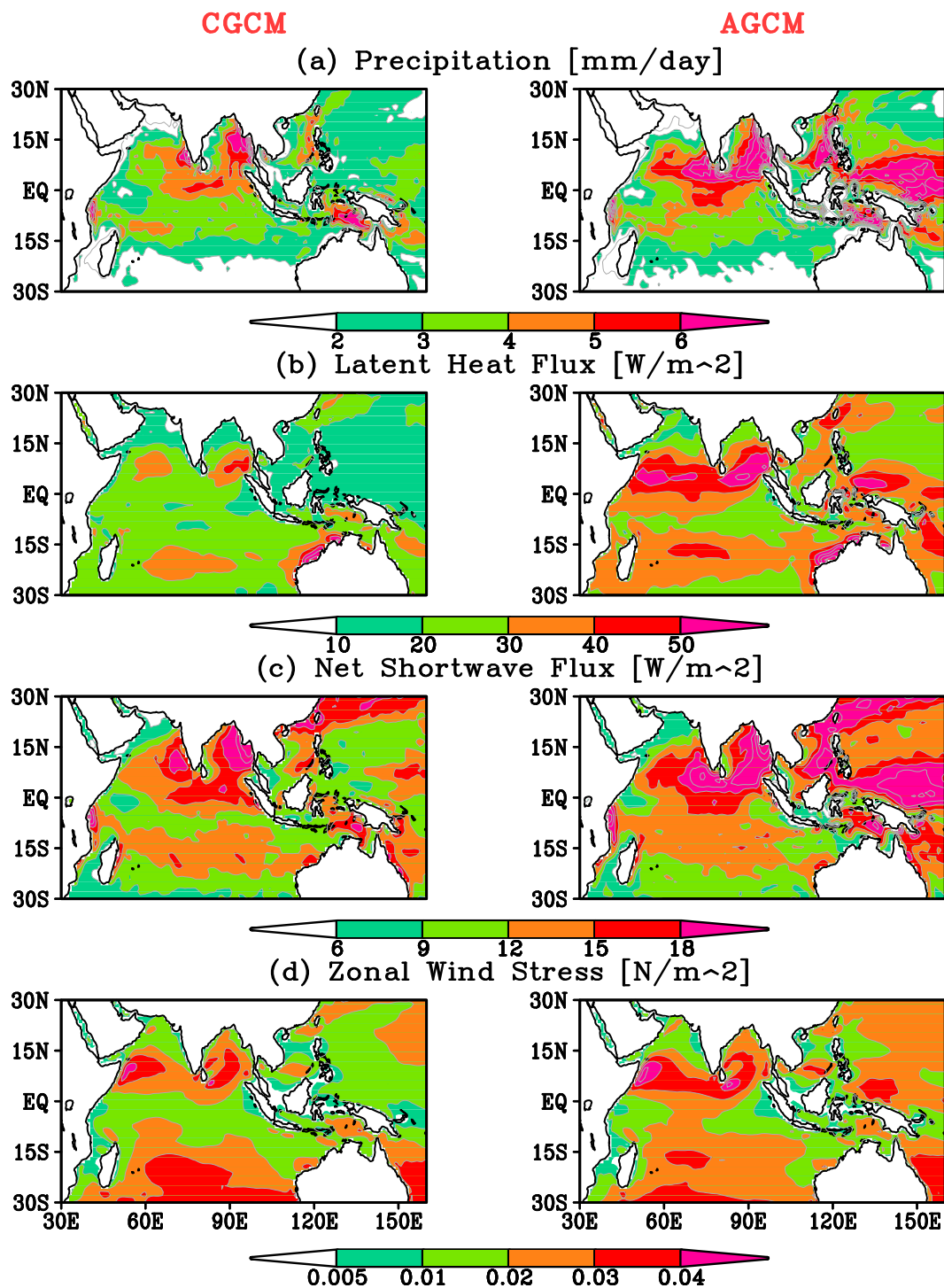


FIG. 1. Standard deviations of full fields in (left) CGCM and (right) AGCM for (a) precipitation (mm day^{-1}), (b) LHF (W m^{-2}), (c) NSWF (W m^{-2}), and (d) Taux (N m^{-2}). All variables are for May corresponding to 1-month lead time.

Standard Deviation of signal Fields (May: 1–Month Lead)

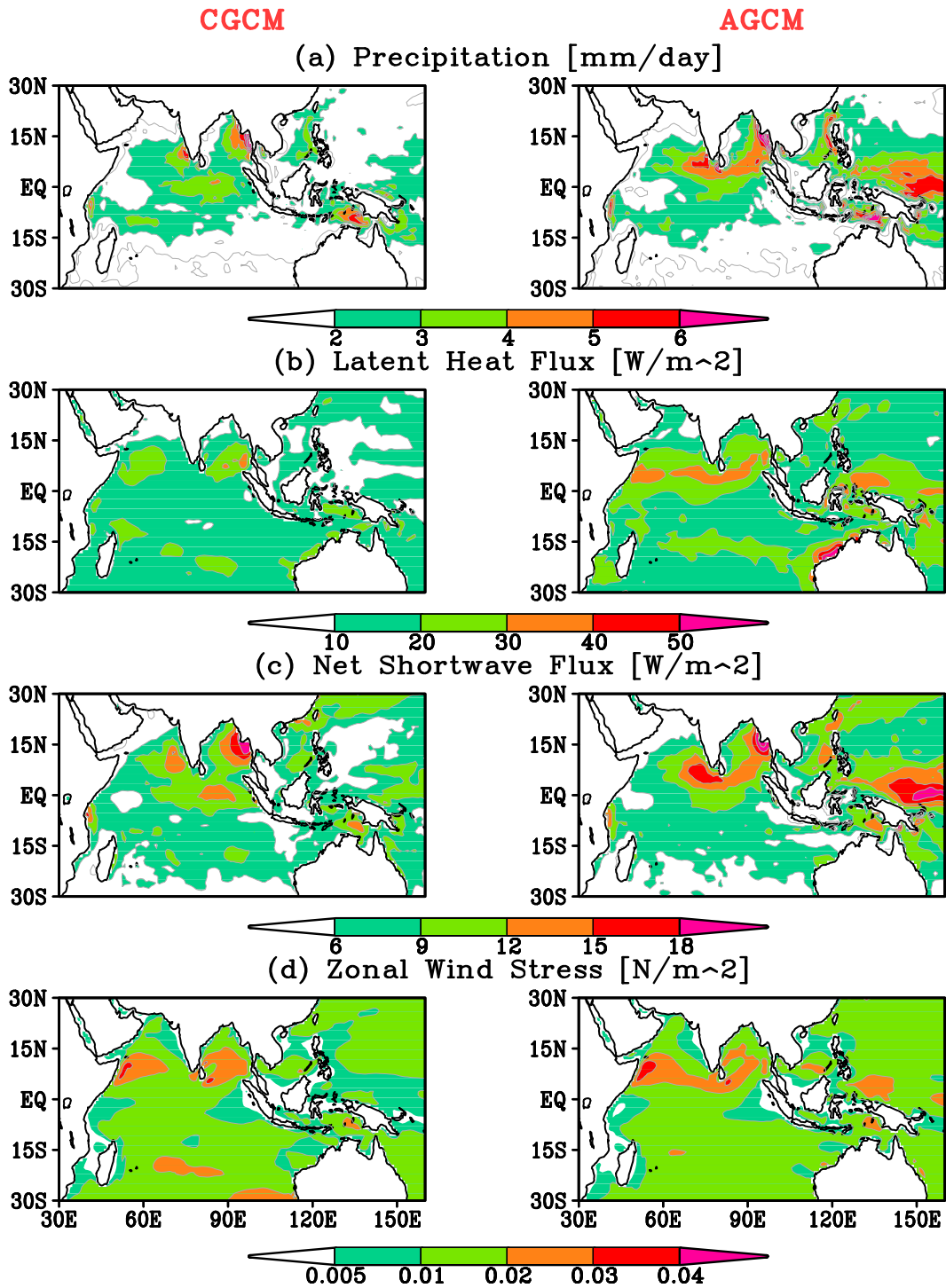


FIG. 2. As in Fig. 1, but for the signal part.

Standard Deviation of noise Fields (May: 1-Month Lead)

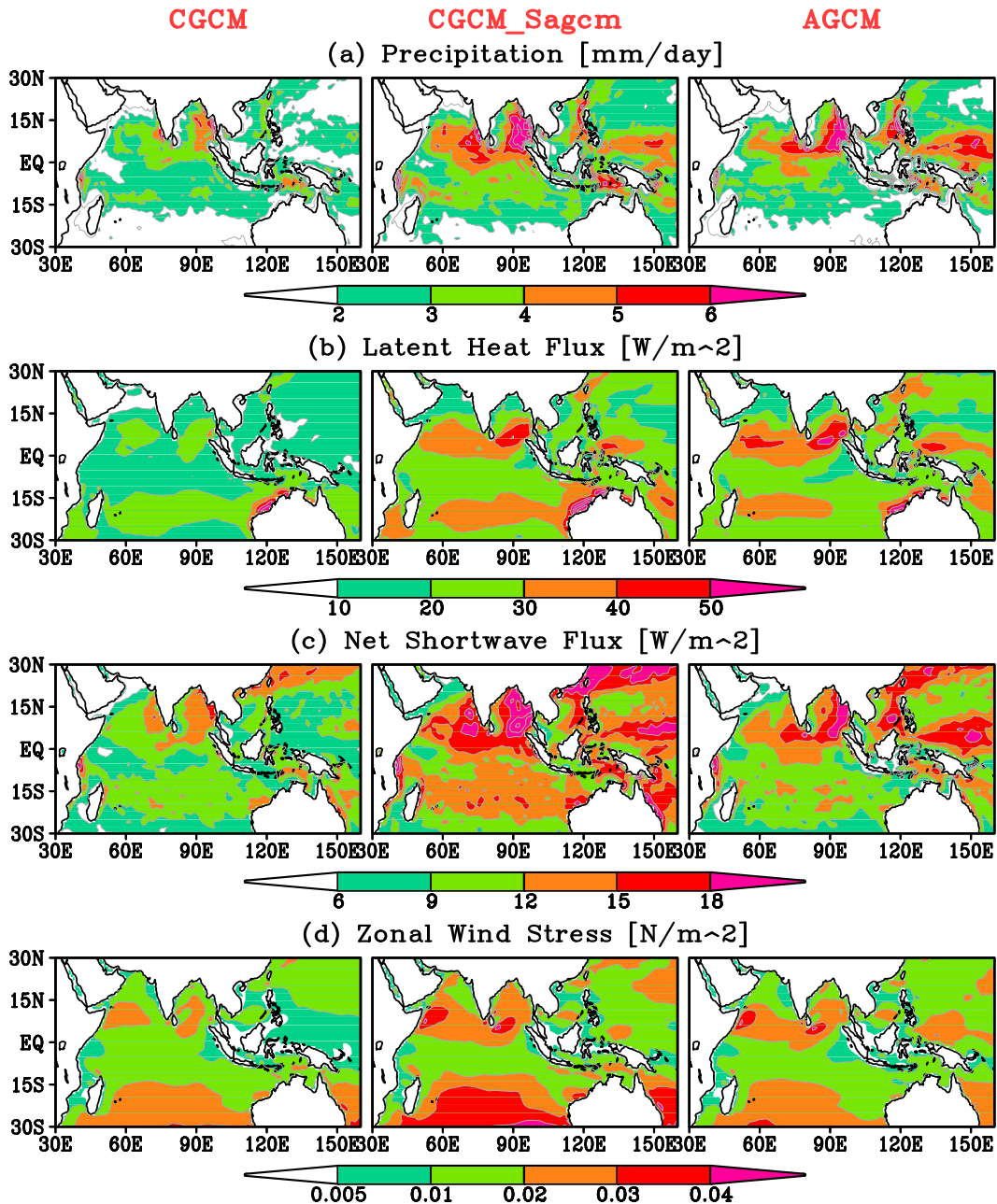


FIG. 3. Standard deviations of the noise part in (left) CGCM, (center) CGCM_Sagcm, and (right) AGCM for (a) precipitation (mm day^{-1}), (b) LHF (W m^{-2}), (c) NSWF (W m^{-2}), and (d) Tau_x (N m^{-2}). The STDs are represented by the average of four STDs from four ensemble members. All variables are for May corresponding to 1-month lead time.

variables. In fact, the similarity appears in most flux variables [see Fig. S1 in the supplemental material for surface sensible heat flux (SHF), net surface longwave flux (NLWF), and meridional surface wind stress (Tau_y)]. It is also noted that the SHF variances (Fig. S1b

in the supplemental material) are not reduced as significantly as other flux variables, which, however, could not change the reduction significance of total fluxes (not shown) because of its minor contributions to total flux in the region. In general, the quantitative significance test

Standard Deviation Ratio: CGCM/AGCM (May: 1-Month Lead)

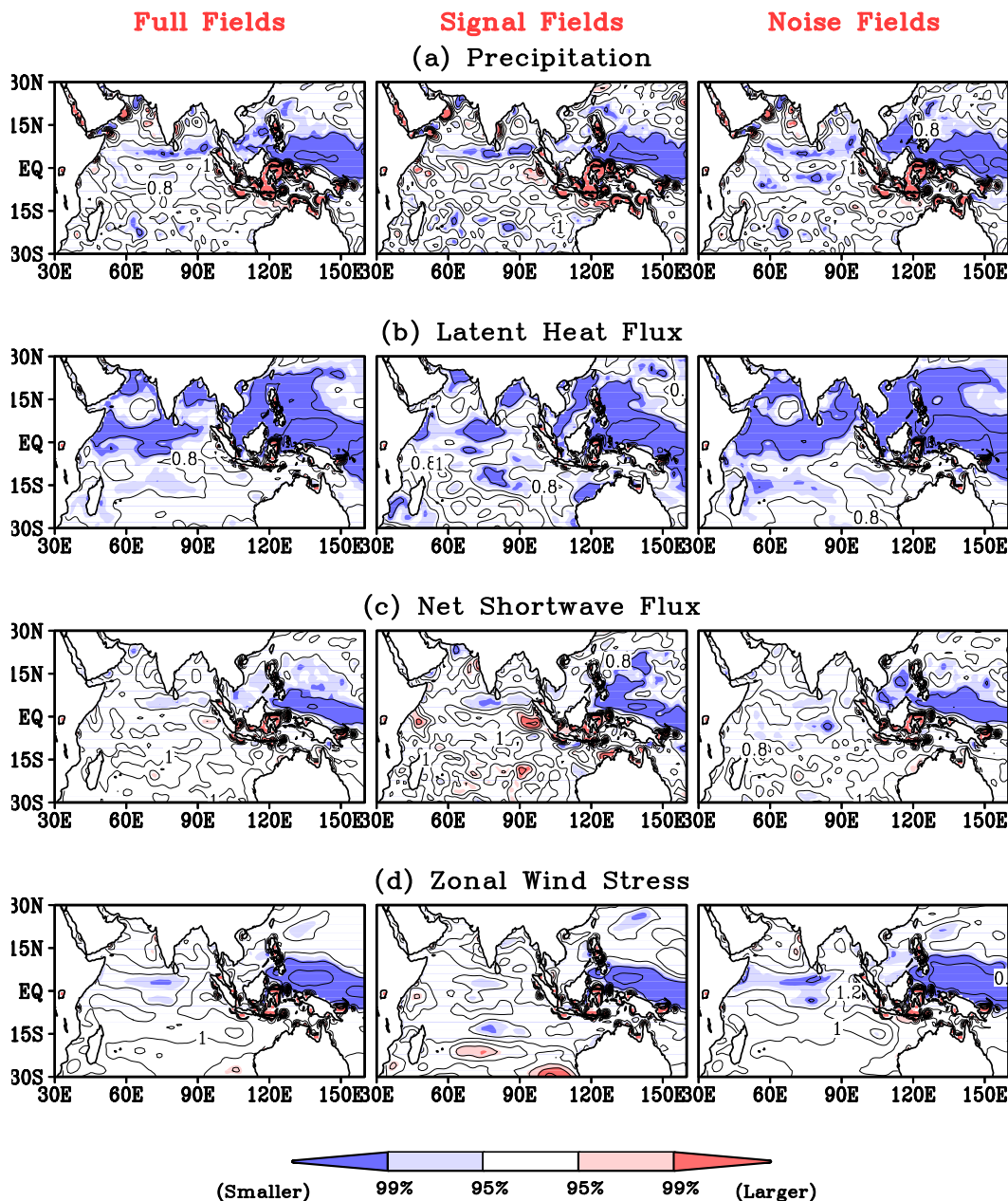


FIG. 4. The ratio of the standard deviations between CGCM and AGCM (CGCM/AGCM) for (left) full fields, (center) the signal part, and (right) the noise part of (a) precipitation, (b) LHF, (c) NSWF, and (d) Taux. All variables are for May corresponding to 1-month lead time. The STDs are represented by the average of four STDs from four ensemble members. The shaded regions represent where the CGCM variance is significantly larger (red) or smaller (blue) than the AGCM variance at the 95% (light colors) and 99% (dark colors) confidence levels according to the F test.

confirms that the variances of full, signal, and noise flux fields are simultaneously reduced as a result of air–sea coupling.

However, if the assumption in the AGCM-based approach (i.e., the signal component is the same between

CGCM and AGCM) is applied in deriving weather noise in both CGCM and AGCM simulations, the noise variance is generally indistinguishable between two simulations (Fig. 5), reproducing the results of Chen et al. (2013). It also suggests that the difference in total

**Standard Deviation Ratio of noise Fields: CGCM_Sagcm/AGCM
(May: 1-Month Lead)**

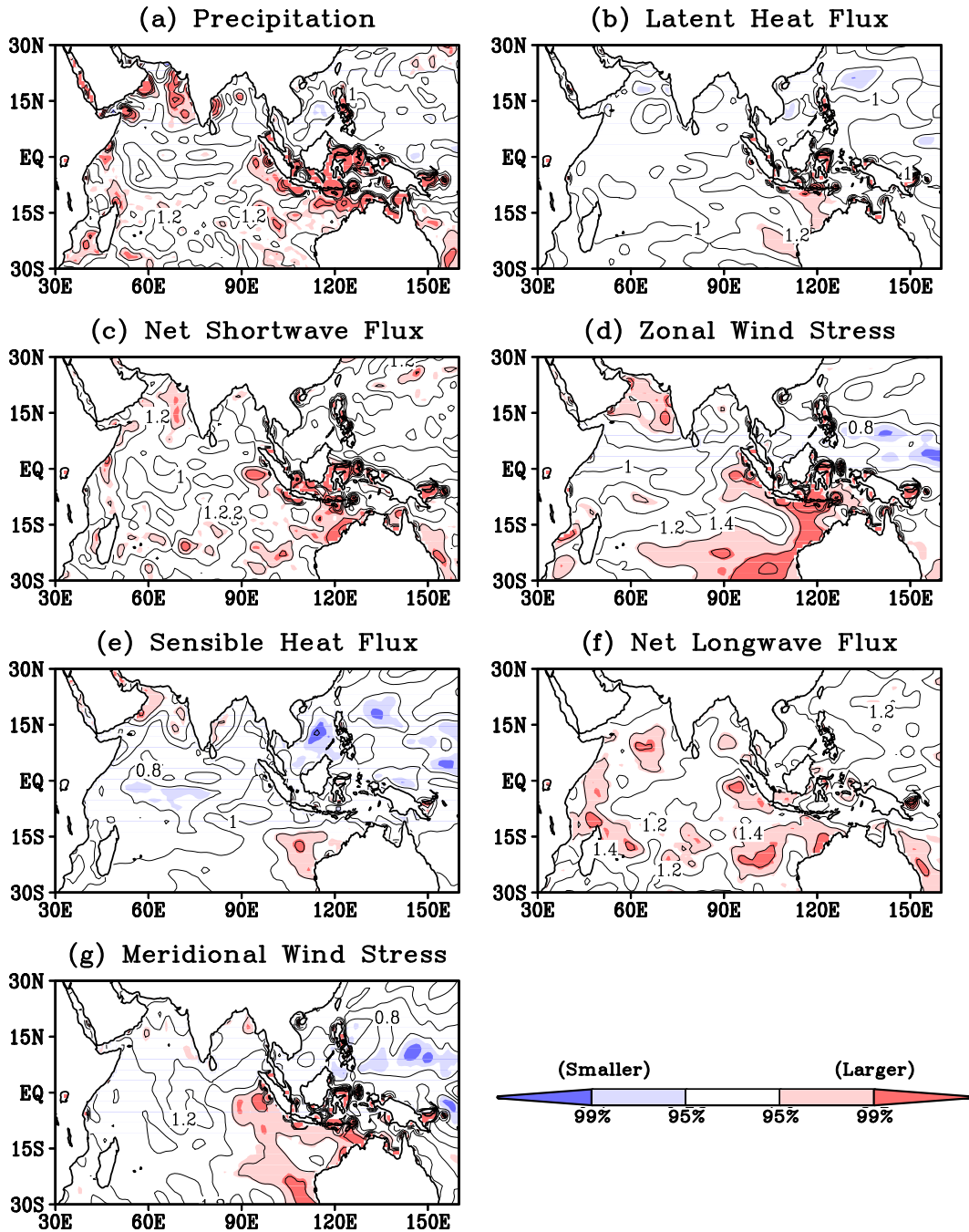


FIG. 5. The ratio of the standard deviations between CGCM_Sagcm and AGCM (CGCM_Sagcm/AGCM) for the noise parts of (a) precipitation, (b) LHF, (c) NSWF, (d) Taux, (e) SHF, (f) NLWF, and (g) Tauy. All variables are for May corresponding to 1-month lead time. The STDs are represented by the average of four STDs from four ensemble members. The shaded regions represent where the CGCM variance is significantly larger (red) or smaller (blue) than the AGCM variance at the 95% (light colors) and 99% (dark colors) confidence levels according to the *F* test.

Standard Deviation Ratio of noise LHF (AGCM_1sst/AGCM)

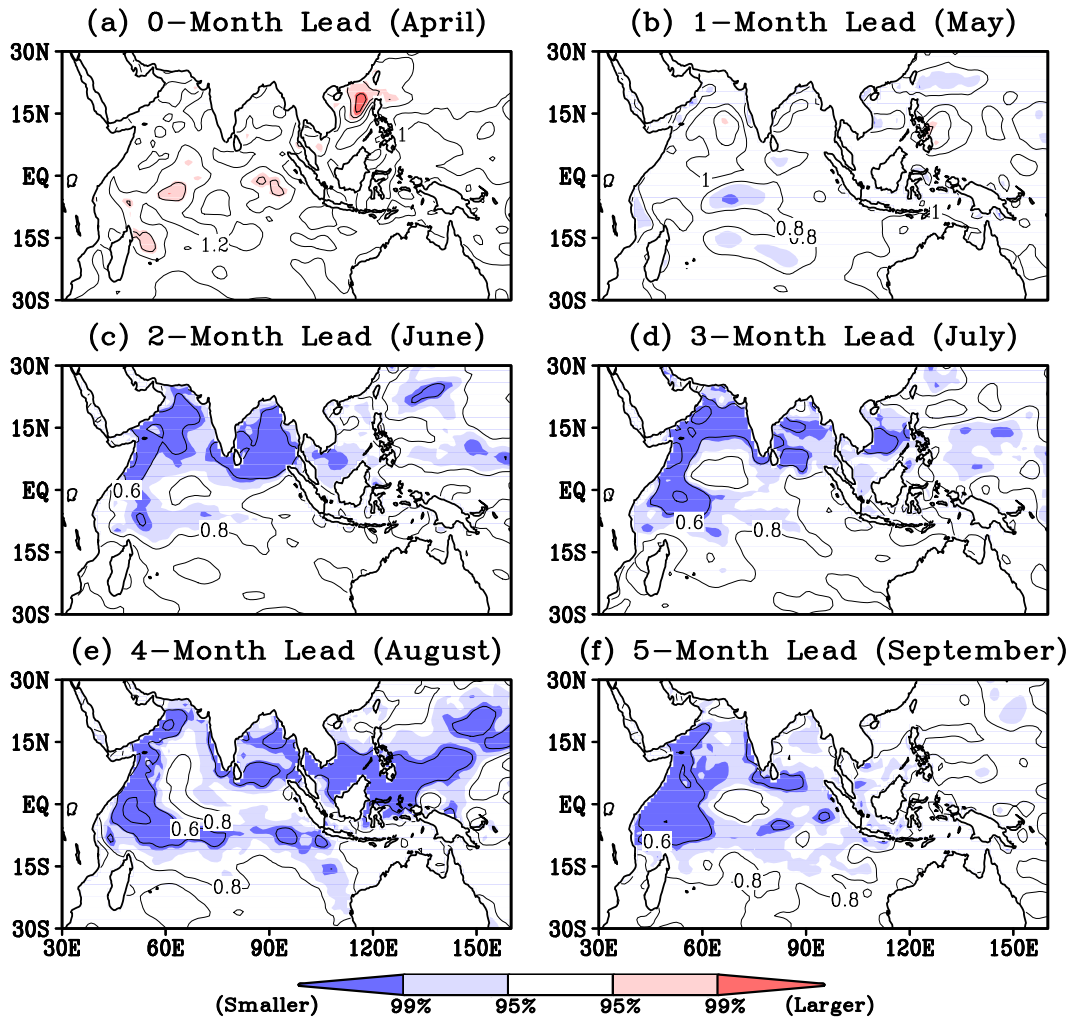


FIG. 6. The ratio of the standard deviations between AGCM_1sst and AGCM ($AGCM_{1sst}/AGCM$) for noise LHF at (a) 0-month lead (April), (b) 1-month lead (May), (c) 2-month lead (June), (d) 3-month lead (July), (e) 4-month lead (August), and (f) 5-month lead (September). The STDs are represented by the average of four STDs from four ensemble members. The shaded regions represent where the CGCM variance is significantly larger (red) or smaller (blue) than the AGCM variance at the 95% (light colors) and 99% (dark colors) confidence levels according to the F test.

variances (Fig. 1) is composed of difference in both signal variances (Fig. 2) and noise variances (Fig. 3).

However, it should be noted that the CGCM-based method using initialized simulations also has a limitation in estimating weather noise because the simulated SST diverges with the increase in lead time (e.g., Zhu et al. 2013), which could increase the variances in the estimated “noise” component. This limitation should be taken into account when the estimated weather noise is used to examine its role in driving low-frequency SST variability (e.g., Schneider and Fan 2007; Fan and

Schneider 2012). Therefore, it will be practically useful to define an efficient period when the SST divergence does not significantly affect the statistics of estimated weather noise (i.e., the CGCM-based method remains valid). For this, AGCM_1sst simulations are conducted, which are forced by the same SST for all members. Figure 6 and supplemental Figs. S2, S3, and S4 present the STD ratio between AGCM_1sst and AGCM for noise LHF, noise precipitation, noise NSWf, and noise Taux, respectively. It is clear that a significant difference appears for all four flux variables at lead times larger than

Standard Deviation Ratio: CGCM/AGCM

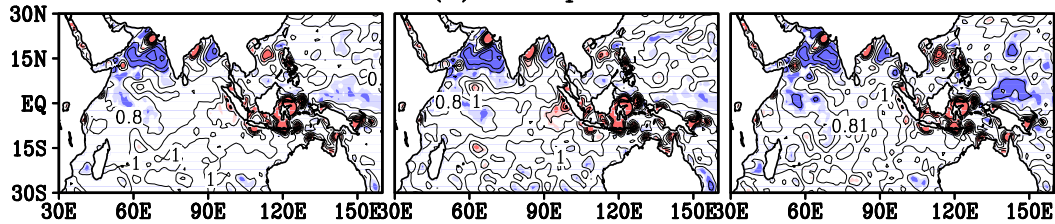
(April: 0-Month Lead)

Full Fields

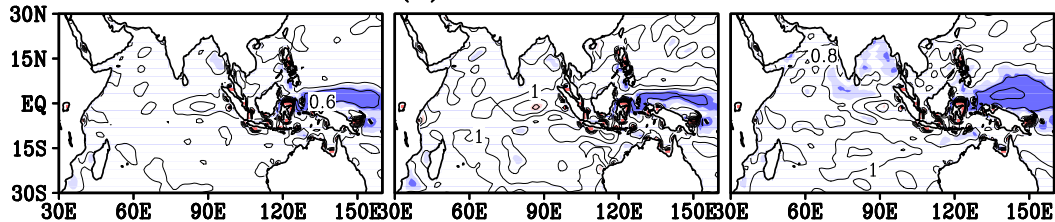
Signal Fields

Noise Fields

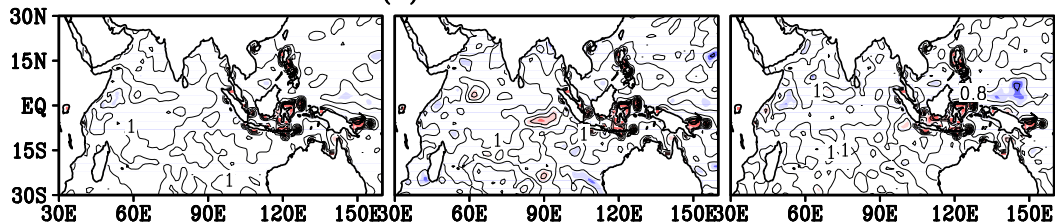
(a) Precipitation



(b) Latent Heat Flux



(c) Net Shortwave Flux



(d) Zonal Wind Stress

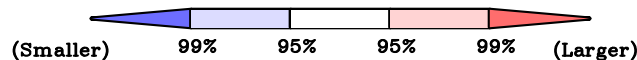
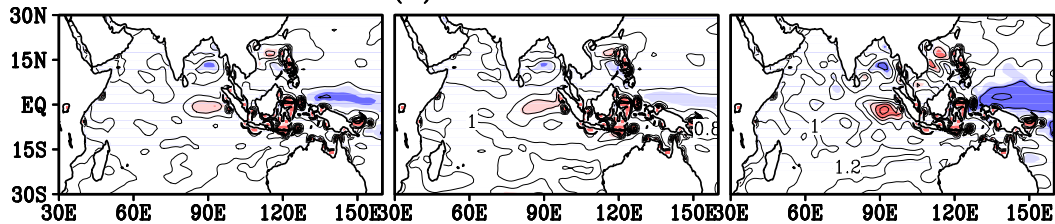


FIG. 7. The ratio of the standard deviations between CGCM and AGCM (CGCM/AGCM) for (left) full fields, (center) the signal part, and (right) the noise part of (a) precipitation, (b) LHF, (c) NSWF, and (d) Taux. All variables are for April corresponding to 0-month lead time. The STDs are represented by the average of four STDs from four ensemble members. The shaded regions represent where the CGCM variance is significantly larger (red) or smaller (blue) than the AGCM variance at the 95% (light colors) and 99% (dark colors) confidence levels according to the F test.

1 month. In particular, at large lead times AGCM has significantly larger noise variances than AGCM_1sst, as expected from the large SST divergence that was included in AGCM simulations. However, at 0- and 1-month lead times, the noise variances are generally not distinguishable

between AGCM_1sst and AGCM. This suggests that for this model, the CGCM-based method would remain valid up to 2 months for estimating weather noise.

Further, the variance difference between AGCM and CGCM has seasonal dependence. Figure 7 presents the

Standard Deviation of noise Precipitation

(JJAS Average: 2~5-Month Leads)

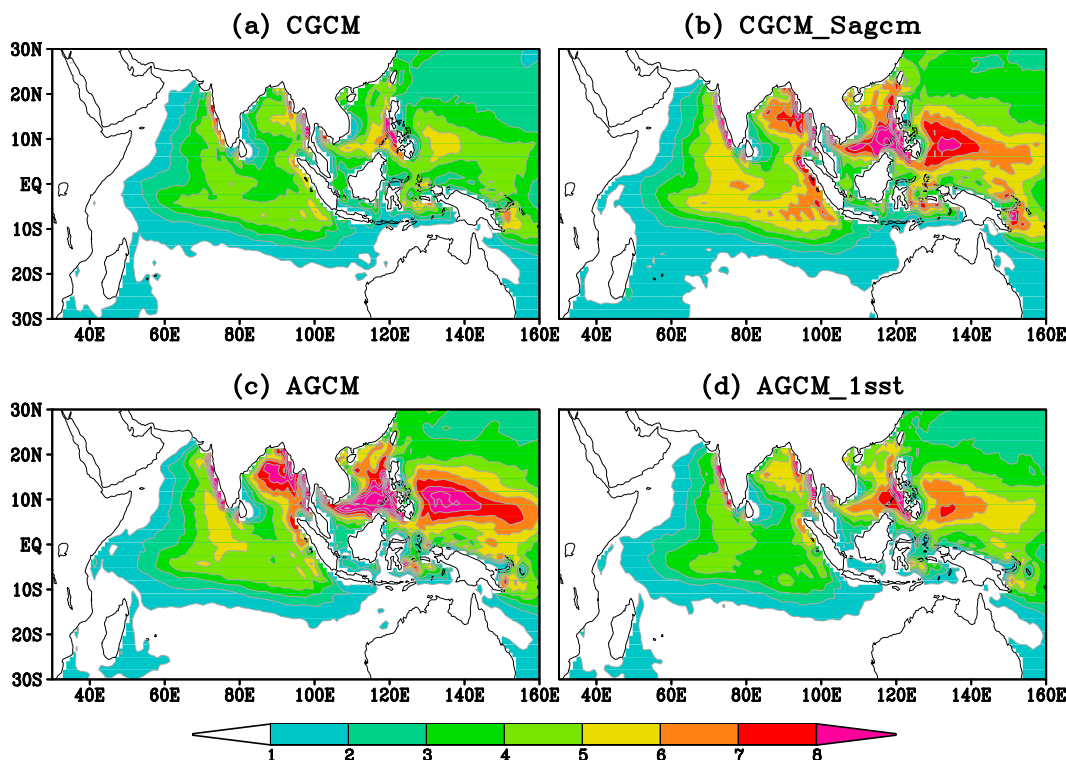


FIG. 8. Standard deviations of noise precipitation (mm day^{-1}) in (a) CGCM, (b) CGCM_Sagcm, (c) AGCM, and (d) AGCM_1sst. The STDs are represented by the average of 16 STDs from four ensemble members during four months (i.e., June–September, corresponding to ~ 2 –5-month lead times).

STD ratio in April (the STD ratio for May was already shown in Fig. 4). The difference between AGCM and CGCM stays consistent among full, signal, and noise fields, but the variance reduction due to air–sea coupling in April is clearly less significant than that in May (Fig. 4). This seasonal dependence corresponds to the seasonality in local air–sea interaction (e.g., rainfall–SST correlation; Wu and Kirtman 2007). For example, over the TWP, the negative rainfall–SST correlation increases from boreal spring to boreal summer [see Fig. 1 in Wu and Kirtman (2007)], and, correspondingly, the variance reduction also increases from April (Fig. 7) to May (Fig. 4) and further to boreal summer (e.g., Fig. 8).

In addition, Fig. 8 also confirms the above noise-related findings derived from our experiments: 1) air–sea coupling reduces the noise variance (Fig. 8a vs Fig. 8c), and 2) the noise variance is generally not distinguishable between CGCM and AGCM if it is assumed that the signal component is the same between them (Fig. 8b vs Fig. 8c), a result consistent with Chen et al. (2013). However, at the long lead times, the noise

variance has a large portion influenced by SST divergence (Fig. 8c vs Fig. 8d).

4. Conclusions and discussion

Schneider and Fan (2007) presented an AGCM-based method to estimate weather noise. This was a major advancement over previous statistical methods (e.g., Kleeman and Moore 1997; Eckert and Latif 1997). As an extension of the dynamical method of Schneider and Fan (2007), this study presents a new method to estimate atmospheric weather noise from coupled models, which is based on initialized simulations with a coupled atmosphere–ocean general circulation model (CGCM). In this method, the weather noise is estimated by removing the signal determined from the coupled ensemble. Compared with the AGCM-based method, the CGCM-based method has the advantage of realistically accounting for air–sea coupling and does not make the a priori assumption that signal variances are the same for coupled and uncoupled simulations.

The model used in this study is the Climate Forecast System, version 2 (CFSv2), the current operational climate prediction model for seasonal-to-interannual prediction at NCEP. The initialized simulations start from each April during 1982–2009 paired with four members and extend for 6 months. To further make a clear comparison between weather noises in coupled and uncoupled simulations, a set of uncoupled AGCM (the atmospheric component of CFSv2) simulations are conducted, which are forced by the daily mean SSTs from the above initialized CGCM simulations. The comparison indicates that, over the Asia–Pacific monsoon region where the local air–sea coupling is important, the noise variances are generally reduced as a result of air–sea coupling, similar to the total and signal variances. The variance difference also exhibits a clear seasonality, with larger difference over the monsoon region appearing toward boreal summer. In addition, since SSTs in the initialized CGCM simulations diverge with the increase in lead time (e.g., [Zhu et al. 2013](#)), it is practically useful to define an “efficient period” when the SST divergence does not significantly affect the statistics of estimated weather noise. Thus, another set of AGCM experiments forced by the same SST is conducted. It is suggested that the CGCM-based method generally remains valid in estimating weather noise within 2 months from its initial start, with little effect from SST divergence.

In summary, these experiments suggest that air–sea coupling generally reduces the variances of flux variables including precipitation, which are simultaneously accompanied by reduced variances in their signal and noise components. In other words, the reduced total variances by air–sea coupling could be due to reductions in both signal variances and noise variances. In fact, in the regions where SST variability is primarily driven by atmospheric forcing, AGCM simulations cannot be realistic and tend to produce a bias toward positive feedback and increase the variances of air–sea fluxes ([Frankignoul 1999](#)). This process could happen on various time scales (e.g., [Chen and Qin 2016](#)), and, correspondingly, the same variance changes by air–sea coupling may appear in both signal and noise fields as defined on the seasonal time scale. On the other hand, the relative strength of changes in signal variances versus those in noise variances reflects predictability changes due to air–sea coupling, which is beyond the scope of this study but will be explored in future.

This study is the first step using a coupled model to quantify what fractions of regional SST variability are driven by weather noise. In future studies, the derived noise fluxes from CGCM could be used to force an interactive ensemble CGCM ([Kirtman and Shukla 2002](#)),

as conducted by [Schneider and Fan \(2007\)](#) and [Fan and Schneider \(2012\)](#).

Acknowledgments. We thank Drs. E. K. Schneider, B. Huang, A. Kumar, P. Peng, Z.-Z. Hu, J. Kinter, and H. Chen for their constructive comments and insightful suggestions. We are grateful to Dr. M. A. Balmaseda from ECMWF for providing its ocean initial conditions and L. Marx for help in the experiment setup. Thanks also go to three anonymous reviewers for their helpful comments. Funding for this study was provided by NSF (AGS-1338427), NOAA (NA14OAR4310160), and NASA (NNX14AM19G). Zhu is also thankful for the Open Project of Key Laboratory of Meteorological Disaster of Ministry of Education (KLME1404), the NSF of China under Grant 41575102, and the project funded by the Priority Academic Program Development (PAPD) of Jiangsu Higher Education Institutions. Computing resources provided by the NASA Advanced Supercomputing (NAS) division are also gratefully acknowledged.

REFERENCES

- Balmaseda, M., K. Mogensen, and A. Weaver, 2013: Evaluation of the ECMWF ocean reanalysis ORAS4. *Quart. J. Roy. Meteor. Soc.*, **139**, 1132–1161, doi:[10.1002/qj.2063](#).
- Barsugli, J. J., and D. S. Battisti, 1998: The basic effects of atmosphere–ocean thermal coupling on midlatitude variability. *J. Atmos. Sci.*, **55**, 477–493, doi:[10.1175/1520-0469\(1998\)055<0477:TBEAO>2.0.CO;2](#).
- Chen, G., and H. Qin, 2016: Strong ocean–atmosphere interactions during a short-term hot event over the western Pacific warm pool in response to El Niño. *J. Climate*, **29**, 3841–3865, doi:[10.1175/JCLI-D-15-0595.1](#).
- Chen, H., E. K. Schneider, B. P. Kirtman, and I. Colfescu, 2013: Evaluation of weather noise and its role in climate model simulations. *J. Climate*, **26**, 3766–3784, doi:[10.1175/JCLI-D-12-00292.1](#).
- Eckert, C., and M. Latif, 1997: Predictability of a stochastically forced hybrid coupled model of El Niño. *J. Climate*, **10**, 1488–1504, doi:[10.1175/1520-0442\(1997\)010<1488:POASFH>2.0.CO;2](#).
- Fan, M., and E. K. Schneider, 2012: Observed decadal North Atlantic tripole SST variability. Part I: Weather noise forcing and coupled response. *J. Atmos. Sci.*, **69**, 35–50, doi:[10.1175/JAS-D-11-018.1](#).
- Frankignoul, C., 1999: A cautionary note on the use of statistical atmospheric models in the middle latitudes: Comments on “Decadal variability in the North Pacific as simulated by a hybrid coupled model.” *J. Climate*, **12**, 1871–1872, doi:[10.1175/1520-0442\(1999\)012<1871:ACNOTU>2.0.CO;2](#).
- , and K. Hasselmann, 1977: Stochastic climate models, Part II. Application to sea-surface temperature anomalies and thermocline variability. *Tellus*, **29A**, 289–305, doi:[10.1111/j.2153-3490.1977.tb00740.x](#).
- Hasselmann, K., 1976: Stochastic climate models. Part I: Theory. *Tellus*, **28A**, 473–485, doi:[10.1111/j.2153-3490.1976.tb00696.x](#).
- Kirtman, B. P., and J. Shukla, 2002: Interactive coupled ensemble: A new coupling strategy for CGCMs. *Geophys. Res. Lett.*, **29**, 1367, doi:[10.1029/2002GL014834](#).

- Kleeman, R., and A. M. Moore, 1997: A theory for the limitation of ENSO predictability due to stochastic atmospheric transients. *J. Atmos. Sci.*, **54**, 753–767, doi:[10.1175/1520-0469\(1997\)054<0753:ATFTLO>2.0.CO;2](https://doi.org/10.1175/1520-0469(1997)054<0753:ATFTLO>2.0.CO;2).
- Saha, S., and Coauthors, 2010: The NCEP Climate Forecast System Reanalysis. *Bull. Amer. Meteor. Soc.*, **91**, 1015–1057, doi:[10.1175/2010BAMS3001.1](https://doi.org/10.1175/2010BAMS3001.1).
- , and Coauthors, 2014: The NCEP Climate Forecast System version 2. *J. Climate*, **27**, 2185–2208, doi:[10.1175/JCLI-D-12-00823.1](https://doi.org/10.1175/JCLI-D-12-00823.1).
- Sarachik, E. S., M. Winton, and F. L. Yin, 1996: Mechanisms for decadal-to-centennial climate variability. *Decadal Climate Variability: Dynamics and Predictability*, D. L. T. Anderson and J. Willebrand, Eds., NATO Advanced Science Institutes Series, Vol. 44, Springer, 158–210.
- Schneider, E. K., and M. Fan, 2007: Weather noise forcing of surface climate variability. *J. Atmos. Sci.*, **64**, 3265–3280, doi:[10.1175/JAS4026.1](https://doi.org/10.1175/JAS4026.1).
- Shukla, R., and J. Zhu, 2014: Simulations of boreal summer intra-seasonal oscillation with the Climate Forecast System, version 2, over India and the western Pacific: Role of air–sea coupling. *Atmos.–Ocean*, **52**, 321–330, doi:[10.1080/07055900.2014.939575](https://doi.org/10.1080/07055900.2014.939575).
- Wang, B., Q. Ding, X. Fu, I.-S. Kang, K. Jin, J. Shukla, and F. Doblas-Reyes, 2005: Fundamental challenge in simulation and prediction of summer monsoon rainfall. *Geophys. Res. Lett.*, **32**, L15711, doi:[10.1029/2005GL022734](https://doi.org/10.1029/2005GL022734).
- Wu, R., and B. P. Kirtman, 2004: Impacts of the Indian Ocean on the Indian summer monsoon–ENSO relationship. *J. Climate*, **17**, 3037–3054, doi:[10.1175/1520-0442\(2004\)017<3037:IOTIOO>2.0.CO;2](https://doi.org/10.1175/1520-0442(2004)017<3037:IOTIOO>2.0.CO;2).
- , and —, 2007: Regimes of local air–sea interactions and implications for performance of forced simulations. *Climate Dyn.*, **29**, 393–410, doi:[10.1007/s00382-007-0246-9](https://doi.org/10.1007/s00382-007-0246-9).
- Zhu, J., and J. Shukla, 2013: The role of air–sea coupling in seasonal prediction of Asia–Pacific summer monsoon rainfall. *J. Climate*, **26**, 5689–5697, doi:[10.1175/JCLI-D-13-00190.1](https://doi.org/10.1175/JCLI-D-13-00190.1).
- , B. Huang, L. Marx, J. L. Kinter III, M. A. Balmaseda, R.-H. Zhang, and Z.-Z. Hu, 2012: Ensemble ENSO hindcasts initialized from multiple ocean analyses. *Geophys. Res. Lett.*, **39**, L09602, doi:[10.1029/2012GL051503](https://doi.org/10.1029/2012GL051503).
- , —, M. A. Balmaseda, J. L. Kinter III, P. Peng, Z.-Z. Hu, and L. Marx, 2013: Improved reliability of ENSO hindcasts with multi-ocean analyses ensemble initialization. *Climate Dyn.*, **41**, 2785–2795, doi:[10.1007/s00382-013-1965-8](https://doi.org/10.1007/s00382-013-1965-8).